Attempting to Extract Power from Earth's Rotation: An Experimental Test

Bastiaan Veltkamp and Rinke J. Wijngaarden[*]

Department of Physics and Astronomy, Vrije Universiteit Amsterdam, 1081 HV Amsterdam, Netherlands

A recently proposed method for the extraction of electrical energy from a circuit that is static with respect to the surface of Earth is investigated experimentally. In this method an electrical circuit moves due to Earth's rotation in Earth's magnetic field, and thus is supposed to generate an electromotive force. Our experimental results demonstrate that the proposed method yields voltages more than 3 orders of magnitude smaller than the predicted signal. This discrepancy is explained, and constraints on alternative schemes are briefly considered.

I. INTRODUCTION

Maintaining the energy supply for humankind at its current level, let alone adapting the supply to the future needs of humankind, is an enormous challenge [1]. Fossil fuels will be phased out soon, both because of limited reserves and to stop a further enhancement of CO_2-induced global warming. Unfortunately, there is currently no simple or single replacement [2]. Therefore, many parallel strategies must be developed. A scheme for the extraction of energy from Earth's rotation using an electromagnetic device was recently proposed by Chyba and Hand [3]. If a power of 10 TW (the present global energy use is of that order of magnitude) is generated with this method, it would "only" quadruple the natural slowing down of Earth's rotation rate. Apart from large-scale applications, their method would be ideal for distributed or remote electronics [4] since this method of generating electricity would need no supply of fuel or mechanical energy.

One main assumption in Ref. [3] is that Earth's magnetic field does not corotate with Earth. This assumption is justified by a series of intriguing experiments by Barnett [5,6] that seem to show that a wire (properly oriented) becomes electrically polarized if it rotates in a static magnetic field, while it does not become polarized if it is static and the magnet rotates. Such difference in behavior between systems that rotate with respect to each other is well known in mechanics from Newton's rotating bucket [7,8] and in electromagnetism from the Sagnac effect [9]. Nevertheless, this particular inequivalence is still intriguing today, as is evident from recent studies [10–13], one of which [11] seems to contradict the result obtained by Barnett and concludes that Earth's magnetic field *is* corotating with Earth.

The main idea presented in Ref. [3] is that an electromotive force (emf) can be developed in a circuit that

is corotating with Earth's surface because such a circuit moves in the presence of the noncorotating magnetic field of Earth. The present paper first reviews this idea in more detail and discusses the instrument (henceforth called the "antenna") Chyba and Hand propose for electricity generation. Then our experimental investigations of their prediction are presented. These do not confirm the predicted effect. We discuss whether experimental flaws could lead to a false negative outcome. Also we revisit the assumptions made in Ref. [3] and conclude that the antenna is not expected to work, in agreement with our observation. Finally, we discuss whether modifications could be made to make the antenna work.

II. EMF AND SHIELDING

Before further discussing the idea in Ref. [3], we present a few remarks on the concept of emf. As is well known [14], a charge q moving with velocity $\mathbf{v}$ in the presence of an electric field $\mathbf{E}$ and a magnetic field $\mathbf{B}$ experiences a Lorentz force $\mathbf{F}_L = q\,(\mathbf{E} + \mathbf{v} \times \mathbf{B})$. In electromagnetic induction, electrical energy is introduced into a circuit by an external source. The work done by the external source per unit of charge in the circuit is the emf $\mathcal{E}$. The value of $\mathcal{E}$ is given (for a discussion, see [14–16]) by

$$\mathcal{E} = \frac{1}{q} \oint_C \mathbf{F}_L \cdot d\mathbf{l} = \oint_C (\mathbf{E} + \mathbf{v} \times \mathbf{B}) \cdot d\mathbf{l}. \qquad (1)$$

In the well-known configuration of a fixed loop *ABCD* shaped as in Fig. 1(a) placed in a perpendicular magnetic field $\mathbf{B}$ and short-circuited through sliding contacts by the moving rod *EF*, a current is generated in the circuit $E'BCF'E'$. In this case, the actor that moves the wire performs work and thus provides the electrical energy.

On the other hand, if a fixed loop *ABCD* moves through a static field [17], as in Fig. 1(b), no current flows. This is
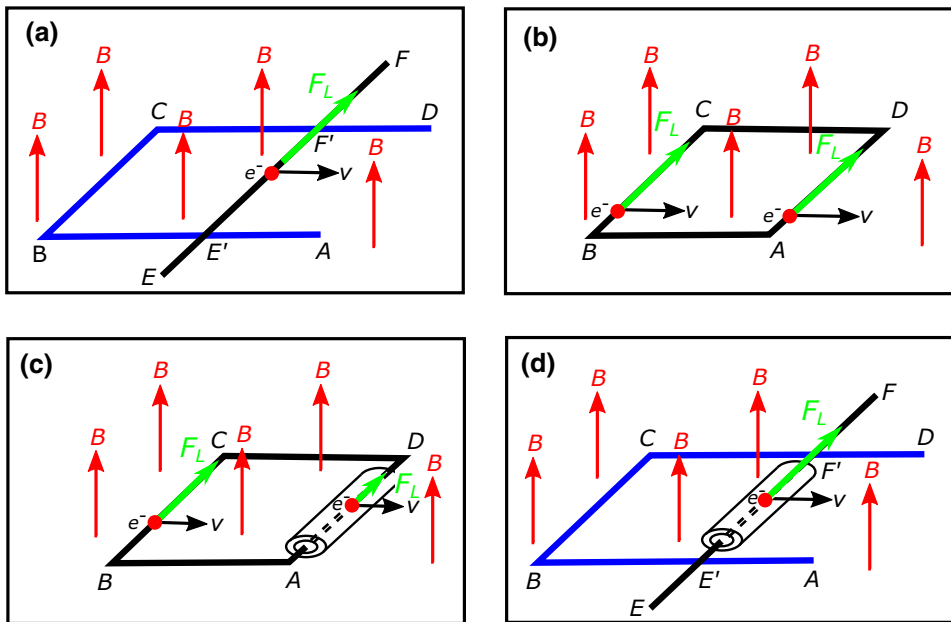
---

[*]rw@nat.vu.nl

FIG. 1. Various configurations to investigate the production of emf, as discussed in the text. In all cases, the red arrows indicate the direction of a uniform magnetic field **B**. The blue lines [in (a),(d)] represent conductors that are static, while the black lines represent conductors moving with velocity **v**, as indicated by the black arrows. The cylinder in (c),(d) is co-moving with and ideally shielding the wire that passes through its center. The Lorentz force $\mathbf{F}_L$ is in the direction of the green arrows.

because the contributions to the circular integral in Eq. (1) along *BC* and *DA* cancel. Locally, however, the Lorentz force leads to a polarization along legs *BC* and *AD*, setting up an electric field **E** that exactly nullifies **v** × **B**. For a further discussion, see Refs. [18,19]. To obtain an emf nevertheless, one could try to avoid the canceling of the contributions to the emf along legs *BC* and *AD* by creating a difference in the local magnetic field **B**, for example, in the manner indicated in Fig. 1(c), where the leg *AD* is magnetically shielded by a co-moving shield, thus reducing **B** at the position of the wire *AD*. Naively, (but falsely) this would result in a nonzero emf $\mathcal{E}$. The antenna proposed in Ref. [3] has another configuration but uses a similar difference of the local magnetic field.

III. PREDICTED EMF

The antenna proposed in Ref. [3] is placed statically with respect to the surface of Earth, which implies that it moves at large velocity with respect to Earth's magnetic field **B**, because this field is supposed (as mentioned) not to be corotating with Earth. Our experimental realization of the antenna is shown in Fig. 2. It consists of a cylindrical shell (a tube with finite thickness) and an electrical circuit consisting of a voltmeter connected either to points *A* and *C* of the tube (as suggested in Ref. [3], and labeled "copper-ferrite circuit" below) or to the ends of a hairpin copper-wire loop as indicated in red in Fig. 2 (labeled "copper-only circuit" below).

In a careful and detailed calculation, based on arguments involving the diffusion of the vector field **A** (with **B** = ∇ × **A**), it is argued in Ref. [3] that **B** has different values at the leading and trailing sides of the shell, thus

generating the desired asymmetry and an emf. Of course, the emf increases with increasing asymmetry of **B**. Thus a material with high permeability is desired, while subtler arguments [3] lead to the constraint $R_m \ll 1$, with $R_m \simeq \sigma \mu_r \mu_0 vb$, where $v = \omega R \cos\lambda$ and ω is the angular frequency of Earth's rotation, R is the radius of Earth, and λ is the latitude at which the antenna is placed.

Under these conditions, the emf $\mathcal{E}$ is given by Eq. (63) in Ref. [3], which we write (see also the Appendix) as

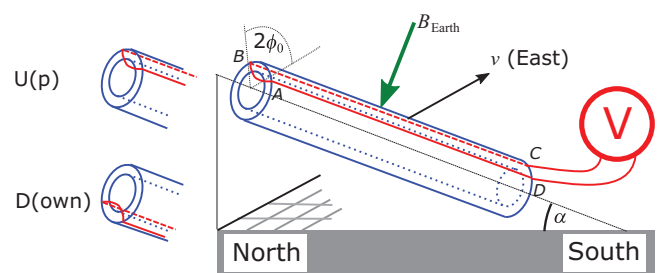$$\mathcal{E} = -\oint_C v B_x \hat{\mathbf{z}} \cdot d\ell, \qquad (2)$$

FIG. 2. The antenna used in our experiment consists of a ferrite tube (blue) that is pointing upward in the direction to the magnetic North at an angle α, as indicated. The voltmeter (V) is directly connected either to two labeled points on the tube, as discussed in the text, or to a copper wire (*DABC*, in red) on the surface of the cylinder as indicated. The full angle (back wire, axis of tube, front wire) is $2\phi_0$. The tube is moving with the surface of Earth to the East at velocity v (thin black arrow) and can be oriented in the up (U) and down (D) configurations. The direction of the local magnetic field of the Earth is indicated by the thick green arrow.

from which—for the geometry of the proposed antenna—one finds

$$\mathcal{E} = 2R_m v \beta_2 \ell \, (a/b)^2 \sin \phi_0 \cos^2 \phi_0, \qquad (3)$$

where a and b are the inner and outer radii of the cylindrical shell and ℓ is the length of the electrical circuit in or on the shell. The angle spanned by the electrical circuit is $2\phi_0$, as indicated in Fig. 2, and

$$\beta_2 = \frac{2B_\infty \mu_r \, (\mu_r - 1)}{(\mu_r + 1)^2 - (a/b)^2 \, (\mu_r - 1)^2} \simeq \frac{2B_\infty}{1 - (a/b)^2}, \quad (4)$$

where the approximate equality holds for large μ_r, and B_∞ is the field of Earth. Also for large μ_r and for the optimal angle $\phi_0 = \arccos \frac{1}{3}\sqrt{6} \approx 35°$, the emf can be approximated as

$$\mathcal{E} = \frac{8}{9}\sqrt{3} B_\infty \sigma \mu_r \mu_0 v^2 \ell \, \frac{a^2 b}{b^2 - a^2}. \qquad (5)$$

In our experiments, the antenna is aligned to the magnetic North with use of a Recta DP6 compass to an accuracy of 2°. According to Ref. [20], the local (at 52.3°N, 4.8°E) magnetic declination is $1.1436° \pm 0.37°$ and the inclination is $67.3057° \pm 0.22°$, while the total magnetic field of Earth is $B_\infty = 49.1462 \, \mu\text{T} \pm 152 \, \text{nT}$. In view of the local inclination, the ferrite tube is oriented at an angle $\alpha = 22.7° \pm 1°$ with respect to the horizontal plane, as indicated in Fig. 2. Since it is predicted in Ref. [3] that the emf changes sign if the antenna is rotated 180°, making the signal distinctive from, for example, thermovoltages, we always measure the difference in voltage ΔV between the up configuration and the down configuration, as shown in Fig. 2. In our copper-ferrite-circuit experiments, the voltmeter is connected to points A and C and thus will detect $\frac{1}{2}\mathcal{E}$, while the expected difference on rotation is $\Delta V = \mathcal{E}$. In the experiments with the copper-wire loop (copper-only circuit), the voltmeter will detect $\mathcal{E}$ and the expected difference on rotation will be $\Delta V = 2\mathcal{E}$. For the parameters mentioned above, Eq. (5) predicts values ΔV values between 1.5 μV and 30 μV for our experiments with different antennas, which should be easily measurable. The experimental results are presented in the following two sections.

IV. EXPERIMENTS WITH A COPPER-FERRITE CIRCUIT

For this experiment, we use a single cable shielding core [21] with $a = 5.07 \pm 0.1$ mm, $b = 9.35 \pm 0.1$ mm, and length $L = 28.6 \pm 0.1$ mm, made from "75" MnZn ferrite [22], mounted on a PVC rod of 10.1-mm diameter. It has conductivity $\sigma = 0.33$ S m^{-1} and relative permeability (in external magnetic fields $\mu_0\mathbf{H} < 1$ mT) $\mu_r = 5000$. At the latitude $\lambda = 52.3°$ of our experiments, this implies $R_m \simeq 5 \times 10^{-3} \ll 1$, satisfying the requirement for the validity of Eq. (5). In agreement with the setup proposed in Ref. [3], copper wires are attached to the ferrite with silver
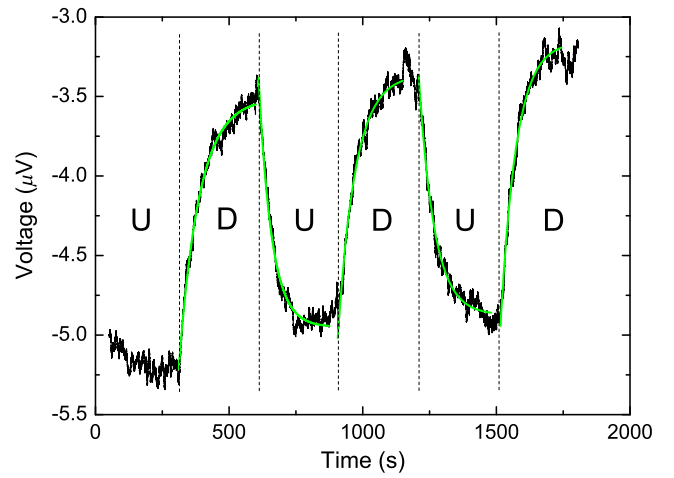

FIG. 3. Voltage obtained with the copper-ferrite circuit. U (up) and D (down) indicate the orientation of the tube (see Fig. 2). Fits obtained with the equation discussed in the text are shown in green. On average they yield a time constant of 61 ± 10 s.

paint at positions corresponding to points A and C shown in Fig. 2. These copper wires are connected to a Keithley 2000 multimeter.

An experiment consists of a repetition of the following cycle: the voltage is recorded during a period of about 300s, then the tube is rotated 180° clockwise, then the voltage is recorded during a period of about 300s, then the tube is rotated 180° counterclockwise. A typical experimental result is shown in Fig. 3, where also the two orientations of the antenna [up (U) and down (D)] are indicated. A voltage difference ΔV of about 1.5 μV is observed, which is roughly the magnitude that is expected from Eq. (5). This seems to support the main idea in Ref. [3]. However, a closer look at Fig. 3 shows that the change in reading on change of the orientation is not instantaneous, but occurs with a time constant τ of 61 ± 10 s, as determined from a set of fits (green lines in Fig. 3) to $V_0 + V_1 \{1 - \exp [-(t - t_0)/\tau]\}$ ($V_0, V_1, t_0,$ and τ are fitting parameters). This time constant τ is certainly not due to the multimeter (which is set to average over 0.2 s) and is larger by several orders of magnitude than any time constant discussed in Ref. [3]. This is the *first* indication that the observed voltage may have a cause different from that proposed in Ref. [3].

In subsequent experiments, with the voltmeter connected to points A and B, about the same change by 1.5 μV is observed. This is striking because according to the theory presented in Ref. [3], and in particular according to Eq. (2), the emf should be zero in this case (we assume no contribution to the emf from the connecting copper wires, as is also assumed in Ref. [3]). On the other hand, with the copper wires connected to points A and D, no change in voltage is detected on rotation by 180°, while Eq. (2) predicts the same emf for connection to A and D or to A

and *C*. In brief, a signal is predicted between *A* and *D* and no signal is predicted between *A* and *B*, while the opposite is observed. This is the *second* deviation with respect to the prediction in Ref. [3].

For $2\phi_0 = \pi$, no signal is predicted between points *A* and *B* due to the angular dependence in Eq. (3), and also since for this path $\hat{\mathbf{z}} \perp \mathbf{d}\ell$ and hence $\mathcal{E} = 0$ according to Eq. (2). However, in our experiment a signal is still observed. This is the *third* deviation found.

The observed discrepancies demonstrate that the signals observed in the experiments discussed above are inconsistent with the effect proposed in Ref. [3]. On the other hand, we conjecture that they can be explained by spurious thermal effects. Indeed, the time constant observed in the experiment for which the results are shown in Fig. 3 matches that observed in heating experiments. In these, the antenna is heated by infrared radiation for times ranging from 2 to 60 s, while the change in voltage is monitored after the heating is switched off. In all cases a decay in the voltage is observed with a time constant of 60 ± 2 s (i.e., the same time constant as observed in the rotation experiments).

Voltages of the order of magnitude as observed in our rotation experiments can be easily thermally generated. The Seebeck coefficient of ferrite can be as high as approximately 1 mV K^{-1} [23,24] (to be compared with, e.g., 5 μV K^{-1} for copper vs tin-lead solder [25]), which means that the observed signals can be explained by changes in the temperature of the ferrite in the millikelvin range on rotation of the antenna. Our setup is enclosed in a expanded polystyrene foam box with 4-cm wall thickness, but we certainly cannot rule out small heating or cooling effects that would systematically lead to a temperature difference between the upper and lower parts of the antenna. Such a temperature difference and hence thermovoltage would be modified in synchrony (albeit with a nonzero time constant) with the rotation of the antenna, hence leading to a spurious up-down difference signal. Heating could occur by nonuniform absorption of (mainly) unidirectional incident radio-frequency electromagnetic radiation or by nonuniform dissipation of radio-frequency currents induced in the tube: the angle between the local magnetization and a current circulating in the ring or tube varies as a function of the position in the ring, possibly leading to nonuniform resistivity due to anisotropic magnetoresistance [26]. Cooling by convection could easily be subject to an asymmetry between the upper side and the lower side of the antenna and thus could also induce such spurious signals.

If the effect proposed in Ref. [3] has a significantly reduced magnitude, it might be hidden by the observed spurious signals. For that reason, experiments are also performed with a copper-only circuit, thus precluding large thermoelectric effects. These experiments are discussed in the next section.

V. EXPERIMENTS WITH A COPPER-ONLY CIRCUIT

Our copper-only circuit is shown as the red circuit in Fig. 2. A loop of copper wire (of 0.4-mm diameter and isolated by an enamel layer about 0.02 mm thick) is carefully mounted with PVC tape on the surface of the ferrite. For practical reasons, the length of the wire ℓ is the same as the length of the tube, i.e. L, contrary to the geometry in Ref. [3], where $\ell < L - 2a$. As a consequence, the use of Eq. (5) will lead to an overestimation of the expected emf (by about 4%). We use the optimal half-opening angle $\arccos \frac{1}{3}\sqrt{6} \simeq 35°$ with an accuracy of about 2°. We stress that although the ferrite is no longer part of the electrical circuit, the emf $\mathcal{E}$ is still given by Eq. (5), as discussed in the Appendix. Our high-permeability tube consists of ten cable shielding cores [27] with $a = 6.4 \pm 0.1$ mm, $b = 12.95 \pm 0.38$ mm, and length 28.6 ± 0.8 mm, each made from the same "75" MnZn ferrite [22] material as discussed above, mounted on a PVC rod of 12.7-mm diameter and pushed closely together such that effectively a ferrite tube with a length L of 286 ± 1 mm is formed. For this tube, $R_m \simeq 7.7 \times 10^{-3}$, satisfying the condition $R_m \ll 1$.

Before our experiment, the cores are individually demagnetized with a commercial demagnetizer. To exclude the effect of local static magnetic fields (e.g., due to magnetized iron in the reinforced concrete of our laboratory), we perform the experiments outdoors in a meadow, located (at 52.30680°N, 4.81730°E) in a large park and thus far from any buildings or metallic structures. To further prevent any electromagnetic interference, electricity (220 V, 50 Hz) for the nanovoltmeter is supplied from a car battery with use of a dc-ac converter. The car is approximately 50 m from the experiment. Data are logged by a laptop computer running on its battery connected by an RS-232 connection to the nanovoltmeter, both at a distance of 2 m from the experiment. The experimental setup is connected by a coaxial wire to the input of the nanovoltmeter. Thus a rotation of the antenna by 180° leads only to a twist in this wire.

To reduce the influence of thermal fluctuations and gradients (which could induce thermovoltages), our setup is enclosed in a expanded polystyrene foam box with 4-cm wall thickness. The nanovoltmeter (which itself is a source of heat dissipation) is located outside this box, but its terminals are protected by another expanded polystyrene foam shield. The thermal shield is rather effective, but some remnant sensitivity to wind-induced temperature fluctuations forced us to discard some of our data.

After some test experiments were done both indoors and outdoors, the results presented here were obtained on December 6, 2017. This was a cloudy day with full cover, and an occasional gust of wind was observed (and recorded in our log). An experiment consists of about ten times the following cycle: the voltage is recorded during a period of

about 20 s, then the tube is rotated clockwise by 180°, then the voltage is recorded during a period of about 20 s, then the tube is rotated counterclockwise by 180°. These voltages are measured with an HP 34420A nanovoltmeter set at its most-sensitive range (1 mV) and set to average over 0.2 s ("NPLC = 10").

During the rotations by 180°, spikes in the voltage are observed due to the change in magnetic flux threading the wire loop. Hence, after each rotation we wait a sufficiently long time (a few seconds) before using the readings. During the experiment, the presence of these spikes confirms that all wires remain properly connected and that the whole circuit is correctly measuring an emf. Also the sign of these spikes nicely alternates with the alternating clockwise and counterclockwise rotation. In the static periods in between the rotations, a dc voltage is expected with polarity alternating between the up configuration and the down configuration and with magnitude given by Eq. (5).

To verify the geometry and correct working of the equipment, we also perform a slow-rotation experiment (0° to 180° in about 15 s) with the nanovoltmeter at a faster setting ("NPLC = 1"), from which we determine experimentally $\int \mathcal{E} dt$ for a rotation by 180°. Noting that

$$\int \mathcal{E} dt = \int \frac{d\Phi}{dt} dt = 2\chi_{\text{eff}} A B_\infty, \tag{6}$$

we can compare the experimental value with the expected value $2\chi_{\text{eff}} A B_\infty \approx 8.2 \times 10^{-7}$ V s, where $\chi_{\text{eff}} \simeq 2$ is the effective susceptibility due to the demagnetization factor of an infinitely long tube [28] oriented perpendicular to the applied field B_∞, while A is the area enclosed by the wire loop. The experimental value deviates at most 30% from the expected value. This deviation and its uncertainty are mainly due to the noisy signal and the inherent difficulty in determining a precise background that compensates for the drift. In any case, the deviation is small enough to have full confidence that the experimental setup is working correctly.

We focus our discussion and explanation on our experiment no. 8 of December 6, 2017. The raw data are shown (red curve) in Fig. 4(a), where "U" (up) and "D" (down) indicate the orientation of our antenna.

The spikes due to the rotation are clearly visibly, while we clearly do not observe the expected difference in emf between the up orientation and the down orientation of nearly 30 μV [from Eq. (5) we expect a difference of 2×15 μV, but as mentioned above, by extension of the wire loop to the full length of the ferrite tube, this voltage is somewhat overestimated]. Clearly, during the course of the experiment a drift of the signal by approximately 200 nV is observed, which we ascribe to thermovoltage. The noise in the raw signal at 7 nV is according to the specifications of the nanovoltmeter for the settings used and is more than 3 orders of magnitude below the expected signal.
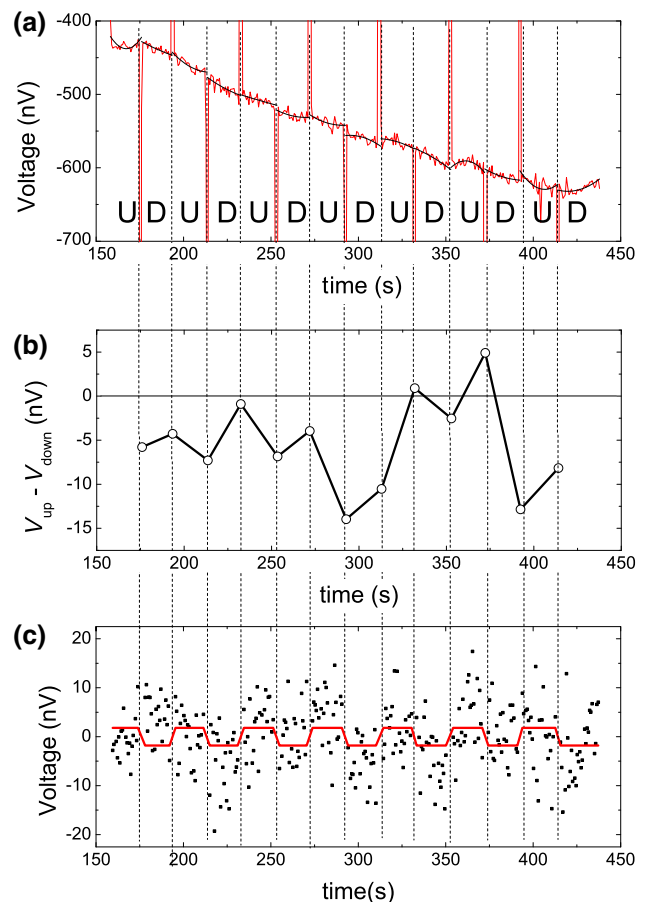

FIG. 4. (a) Experimental data points as measured by the nanovoltmeter (noisy signal, shown in red). The main downward trend is due to drift; the large spikes are due to rotation of the antenna clockwise from the up configuration (U) to the down configuration (D) and counterclockwise from the down configuration to the up configuration. Fits to the data between the spikes are shown in black (smooth curves). (b) Differences between the extrapolated up-configuration and down-configuration fits for each rotation. These differences should correspond to twice the expected dc signal. (c) The raw signal minus a fitted spline (black dots) and the fitted square wave (red line). See the text for details.

For the analysis of the experimental data, we use only the data obtained during periods where there is no rotation and where the rotation-induced spike has sufficiently decayed. We extract the voltage difference between the up orientation and the down orientation by two methods, both intended to accommodate the (thermally induced) drift in the signal.

In the first method, the raw data [red curve in Fig. 4(a)] of each up-orientation period and each down-orientation period are separately fitted to a second-order polynomial. These polynomials [shown as black curves in Fig. 4(a)] are subsequently extrapolated to the midpoints between two successive periods. We define the up-down difference as the difference between the two extrapolations in

the middle of the interval of rotation. This difference is always defined as the extrapolated up-orientation value minus the extrapolated down-orientation value, thus providing an experimental value for the up-down difference. The set of such values as obtained from the data in Fig. 4(a) are presented in Fig. 4(b). The average of the up-down differences is 5.4 ± 5.4 nV (i.e., within the noise we have a zero difference between the up and down orientations). This means that if there is any such effect as predicted in Ref. [3], it is at least 1000 times smaller than predicted.

In the second method, a nonlinear simplex fitting procedure is applied, where the raw data are fitted to a seven-point spline (to accommodate the drift) plus a square wave with amplitude V_0 and a wave form corresponding to the up and down orientations versus time (to model the expected signal). The fit parameters are the voltages at the seven points of the spline and the amplitude V_0. In Fig. 4(c) we show the raw data minus the spline only as black dots and the fitted square wave as a red line. The fit yields $2V_0 = 3.6$ nV for the up-down difference of the expected real signal, also at least 1000 times smaller than predicted.

Both our analyses are consistent with no signal being measured, although we cannot exclude that there is a signal present that is at least 1000 times smaller than the predicted signal. Control experiments indoors show a somewhat smaller drift in the signal but also no statistically significant difference between the up orientation and the down orientation.

VI. DISCUSSION

We conclude that in neither of the two types of experiments presented above, there is a signal observed that is consistent with the predictions in Ref. [3]. There may be various reasons for this. Apart from trivial reasons (such as faulty equipment, which we have ruled out by the checks detailed above) these are (i) Earth's field is corotating with Earth and (ii) the ferrite tube does not have the predicted effect on the emf. In the next paragraphs, we argue that the ferrite tube does not create the asymmetry needed for the predicted emf. Of course, this leaves open the possibility that also reason (i) applies.

To argue that the ferrite tube does not create the desired asymmetry in the magnetic field, we first present a paradox. Consider the textbook situation of a static U-shaped wire that is situated in a plane perpendicular to a uniform magnetic field $\mathbf{B}_e$; see Fig. 1(a). A linear rod is in electrical contact with both legs of the U and moves with constant velocity $\mathbf{v}$ to the right. In this situation, one argues macroscopically that the flux Φ enclosed by the loop is increasing linearly with time and hence creates a nonzero emf $\mathcal{E} = (d\Phi/dt) \neq 0$. Also microscopically, a nonzero emf is found: the Lorentz force on charge carriers in the

moving wire is $\mathbf{F}_L = \mathbf{v} \times \mathbf{B}_e \neq 0$ and is not balanced by another (Lorentz) force in any part of the circuit.

Now a tube of ferrite is added around the moving wire [29] [see Fig. 1(d)] and perfect magnetic shielding is assumed (i.e., the magnetic field $\mathbf{B}_w$ at the wire is given by $\mathbf{B}_w = \mathbf{B}_e + \mathbf{B}_t = 0$, where $\mathbf{B}_t$ is field at the wire due to the magnetization of the tube). In this case, there is macroscopically still a nonzero emf $\mathcal{E} = (d\Phi/dt) \neq 0$. However, microscopically we naively find $\mathbf{v} \times \mathbf{B}_w = 0$, because $\mathbf{B}_w = 0$, and hence a zero Lorentz force, which contradicts the macroscopic argument. The resolution of this paradox is that the co-moving tube does not change the emf or the Lorentz force [30,31] as we now demonstrate.

The Lorentz force is independent of the inertial frame in which it is observed and can be calculated from $\mathbf{F}_L = q\,(\mathbf{E} + \mathbf{v} \times \mathbf{B})$ provided $\mathbf{v}$ is the velocity of the charge q in the same frame where $\mathbf{B}$ and $\mathbf{E}$ are observed [14,32]. On changing from an inertial frame S to another frame S' that is moving with velocity $\mathbf{u}$ with respect to S, the quantities $\mathbf{v}$, $\mathbf{E}$, and $\mathbf{B}$ change according to the relations given in Refs. [33,34], of which we use $\mathbf{v}' = \mathbf{v} - \mathbf{u}$, $\mathbf{B}' = \mathbf{B}$, and $E'_\perp = (\mathbf{E} + \mathbf{u} \times \mathbf{B})_\perp$, where $\mathbf{u}$ and $\mathbf{v}$ are assumed to be nonrelativistic, the primed symbols refer to S', and the unprimed symbols refer to S, while the perpendicular symbol refers to vector components perpendicular to $\mathbf{u}$. Using these relations, one can calculate $\mathbf{F}_L$ in any frame, provided that $\mathbf{B}$, $\mathbf{E}$, and $\mathbf{v}$ in one frame are already known. In particular, in the rest frame of a coil or permanent magnet that is the source of a magnetic field $\mathbf{B}$, we know that $\mathbf{E}$ is zero [18] (in the absence of other sources of electromagnetism). This is an essential starting point for any application of the Lorentz-force equation. It is not so that the velocity $\mathbf{v}$ is a velocity with respect to the source of the field [19], but rather that in using the Lorentz-force equation, one needs to carefully determine the rest frame of the source of the field, and from there determine what $\mathbf{v}$, $\mathbf{B}$, and $\mathbf{E}$ are in that (and hence in any other) frame. We stress this point because the ignoring of it has given rise to a lot of confusion as discussed in Refs. [19,35].

For the analysis of Fig. 1(d), let S be the reference frame that is static with respect to the hairpin wire (blue) and let S' be the rest frame of the wire EF (black) and the tube (i.e., the frame that is moving at velocity $\mathbf{u} = \mathbf{v}$ with respect to frame S). The subsequent analysis is made in frame S'. In this frame, $\mathbf{v}' = \mathbf{v} - \mathbf{u} = \mathbf{0}$. The "total Lorentz force" can be calculated by summing the Lorentz force due to the external field $\mathbf{F}'_{L,e}$ and the Lorentz force due to the tube $\mathbf{F}'_{L,t}$. To find $\mathbf{F}'_{L,e}$, note that in S' there is an electric field $\mathbf{E}'_e = \mathbf{u} \times \mathbf{B}_e$ due to $\mathbf{B}_e$ and the motion of S' with respect to S. Hence $\mathbf{F}'_{L,e} = q\,(\mathbf{E}'_e + \mathbf{v}' \times \mathbf{B}'_e) = \mathbf{u} \times \mathbf{B}_e = \mathbf{v} \times \mathbf{B}_e$. To find $\mathbf{F}'_{L,t}$, note that $\mathbf{E}'_t = 0$ (S' is the rest frame of the tube) and that $\mathbf{v}' = \mathbf{0}$; hence $\mathbf{F}'_{L,t} = q\,(\mathbf{E}'_t + \mathbf{v}' \times \mathbf{B}'_t) = \mathbf{0}$. Thus, in S', the total Lorentz force is $\mathbf{F}'_L = \mathbf{F}'_{L,e} + \mathbf{F}'_{L,t} = \mathbf{v} \times \mathbf{B}_e$. A similar argument (see also below) in S yields, of course,

the same result: $\mathbf{F}_L = \mathbf{F}'_L = \mathbf{v} \times \mathbf{B}_e$. We conclude that with the ferrite tube the same Lorentz force and hence the same emf is observed as without the tube: *the shielding tube does not have any influence on the emf.*

In the previous paragraph we demonstrated that the ferrite tube in Fig. 1(d) has no influence on the emf. Analogous arguments can be made for the tube in Fig. 1(c) and also for the tube in the antenna in Fig. 2 as is now discussed. First consider the frame K' defined in Ref. [3] as the rest frame of the antenna. The magnetization of the tube gives rise to a magnetic field $\mathbf{B}'_t$ in this frame. The frame K, which is the main frame considered in Ref. [3] and which we also consider here, is moving with velocity $-\mathbf{u}$ with respect to K'. In K, the magnetic field $\mathbf{B}_t = \mathbf{B}'_t$ is also present, and due to the field transformations there is an electric field $E_{t\perp} = (-\mathbf{u} \times \mathbf{B}_t)_\perp$. Apart from this, there is a constant background magnetic flux density $\mathbf{B}_\infty$ in K. In the frame K, the antenna is moving with velocity $\mathbf{v} = \mathbf{u}$ (note that the antenna is static in K' and hence $\mathbf{v}' = \mathbf{v} - \mathbf{u} = 0$, as above) and the Lorentz-force component along the tube $F_{L\perp}$ on a charge q in the tube is found as follows:

$$
\begin{aligned}
F_{L\perp}/q &= E_{t\perp} + (\mathbf{v} \times \mathbf{B})_\perp \\
&= (-\mathbf{u} \times \mathbf{B}_t)_\perp + [\mathbf{v} \times (\mathbf{B}_\infty + \mathbf{B}_t)]_\perp \\
&= (-\mathbf{v} \times \mathbf{B}_t)_\perp + (\mathbf{v} \times \mathbf{B}_\infty)_\perp + (\mathbf{v} \times \mathbf{B}_t)_\perp \\
&= (\mathbf{v} \times \mathbf{B}_\infty)_\perp , \quad\quad (7)
\end{aligned}
$$

where the perpendicular symbol indicates a component perpendicular to $\mathbf{u}$ or equivalently along the antenna. Clearly, for the antenna presented in Ref. [3], the Lorentz-force component $F_{L\perp}$ depends on $\mathbf{v} \times \mathbf{B}_\infty$ only and is not modified by (the magnetization of) the ferrite tube. This is true independent of the amount of shielding and of its structure (the spatial dependence of the magnitude of $\mathbf{B}_t$) and also independent of the cause of the shielding (bound or free currents) and holds independently of the position of the wire where $F_{L\perp}$ acts. It holds even if (part of) the "wire" is the ferrite tube itself.

Since $F_{L\perp}$ is not changed by the tube, also the emf is not changed (note that due to the dot product in Eq. (1), only $F_{L\perp}$ contributes to the emf). This means that—despite the presence of the tube—the antenna in Ref. [3] is equivalent to the circuit in Fig. 1(b), and thus is expected to have zero emf (incidentally, the same conclusion is reached in Ref. [36]). Hence the antenna, as proposed, will not be able to extract power from Earth's rotation, in agreement with our experimental results. We note that in Ref. [3] the magnetic field of the moving tube is given by $\mathbf{B}_0 + \mathbf{B}_1$, where $\mathbf{B}_1$ is due to the motion of the tube. The extra field $\mathbf{B}_1$ can be taken into account, without our conclusion being affected, by use of $\mathbf{B}_t = \mathbf{B}_0 + \mathbf{B}_1$ everywhere in the argument above.

Having ruled out the possibility of creating a net emf by magnetic shielding, one may wonder whether any other

scheme could lead to an emf in a fixed loop that is mounted at a fixed orientation with respect to the surface of Earth. Provided that such a loop can be considered to be moving with respect to Earth's field, this seems indeed not *a priori* impossible. One might, for example, envision a planar loop fixed with respect to the surface of Earth with its normal in the direction of East. The bottom and top parts of the loop are at different heights and thus have different velocities due to their different distances from the center of rotation of Earth, while they are also in different fields $\mathbf{B}$. This could induce the asymmetry needed for a net emf. However, it can be easily verified that there is no emf generated in any (rectangular) planar wire loop located in a plane that also contains the axis of symmetry of a dipolar magnetic field and that rotates around that axis (as is the case for the loop just considered).

The known (mainly diurnal) variations of Earth's magnetic field [37,38] could generate an emf, but with much smaller values than those predicted in Ref. [3] and thus will be of less practical interest. An investigation of other possibilities is left for future work.

VII. CONCLUSION

We investigate experimentally the claim that electrical energy can be extracted from Earth's rotation by the antenna proposed in Ref. [3] and find, unfortunately, that the induced voltage is at least 1000 times smaller than predicted and consistent with zero. Our theoretical refutation of the usefulness of magnetic shielding in this context seems to preclude any scheme that depends on the modification of the magnetic field by a corotating contraption, be it a magnetic or an electromagnetic shield. On the other hand, the possibility of converting rotational energy of Earth into electrical energy by devices not considered here cannot be ruled out *a priori*.

ACKNOWLEDGMENTS

APPENDIX: VALIDITY OF EQ. 5 FOR A WIRE ON THE SURFACE OF THE FERRITE TUBE

In this appendix we demonstrate that—provided the argumentation in Ref. [3] is followed—Eq. (2) and hence Eq. (5) can also be applied to a loop immediately above the ferrite tube, such as the copper-only loop discussed in the main text.

The first equality in Eq. (63) in Ref. [3] for the steady state, with $A_z = A_s$, can be rewritten as follows:

$$\mathcal{E} = -\eta \oint_C \nabla^2 A_z \hat{\mathbf{z}} \cdot d\ell, \qquad (A1)$$

$$\mathcal{E} = -\oint_C v \frac{\partial A_s}{\partial y} \hat{\mathbf{z}} \cdot d\ell, \qquad (A2)$$

$$\mathcal{E} = -\oint_C v B_x \hat{\mathbf{z}} \cdot d\ell, \qquad (A3)$$

where Eqs. (26) and (27) in Ref. [3] are used to obtain Eq. (A2), while Eq. (17) in Ref. [3] is used to obtain Eq. (A3).

To apply Eq. (A3) to a loop immediately above the tube (at the radial position $\rho = b$), B_x at that position is needed. Following Ref. [3], we limit the discussion to the perturbative field B_{1x}, since that field contributes to the emf [see the discussion in Ref. [3] below Eq. (64)]. In the following, first the boundary conditions are discussed, and then these are applied to relate the internal (B^i) and external (B^e) components of B_1.

Because of the continuity of the perpendicular component of $\mathbf{B}$,

$$B_{1\rho}^i = B_{1\rho}^e. \qquad (A4)$$

On the other hand, the parallel field components are decoupled by the (equivalent) surface current density $\mathbf{K}$:

$$\Delta \mathbf{B}_\parallel := \mathbf{B}_\parallel^e - \mathbf{B}_\parallel^i = \mu_0 \left(\mathbf{K} \times \mathbf{n} \right), \qquad (A5)$$

where $\mathbf{n} = (\cos\phi, \sin\phi, 0)$ is the unit vector perpendicular to the surface of the tube.

The surface current density is the sum of the magnetization-related bound currents $\mathbf{K}_b = \mathbf{M} \times \mathbf{n}$ and the free current. The latter is the current flowing in the tube due to the emf and is very much smaller than the bound current. Thus to a very good approximation $\mathbf{K} = \mathbf{K}_b$, and hence

$$\Delta \mathbf{B}_\parallel \simeq \mu_0 \left[(\mathbf{M} \times \mathbf{n}) \times \mathbf{n} \right], \qquad (A6)$$

where the magnetization $\mathbf{M}$ is related to the field $\mathbf{B}$ by $\mu_0 \mathbf{M} = [(\mu_r - 1)/\mu_r] \mathbf{B}$. Thus

$$\Delta \mathbf{B}_\parallel \simeq \left(\frac{\mu_r - 1}{\mu_r} \right) \left[(\mathbf{B} \times \mathbf{n}) \times \mathbf{n} \right]. \qquad (A7)$$

Because of symmetry, $B_z = 0$, while B_{1x} and B_{1y} are specified by Eqs. (60) and (62) in Ref. [3]. Substitution of these

expressions yields

$$\Delta \mathbf{B}_{1\parallel} = \mathbf{B}_{1\parallel}^e - \mathbf{B}_{1\parallel}^i = 0, \qquad (A8)$$

and in particular

$$\Delta B_{1\phi} = B_{1\phi}^e - B_{1\phi}^i = 0. \qquad (A9)$$

Since according to Eq. (D4b) in Ref. [3] $B_{1\phi}^i = 0$, we find immediately outside the tube

$$B_{1\phi}^e = 0. \qquad (A10)$$

From Eq. (D4a) in Ref. [3] and in view of Eq. (A4), the external radial field component is given by

$$B_{1\rho}^e \left(\rho \lessgtr b \right) = -\frac{1}{2} R_m b^{-2} \beta_2 a^2 \sin 2\phi. \qquad (A11)$$

Finally, B_{1x}^e is found by substitution of Eqs. (A11) and (A10) into the inverse of Eq. (D1) in Ref. [3]:

$$B_{1x}^e \left(\rho \gtrless b \right) = -B_{1\phi}^e \sin\phi + B_{1\rho}^e \cos\phi, \qquad (A12a)$$

$$B_{1x}^e \left(\rho \gtrless b \right) = -R_m b^{-2} \beta_2 a^2 \sin\phi \cos^2\phi. \qquad (A12b)$$

Thus B_{1x} has exactly the same functional form outside [Eq. (A12b)] and inside [Eq. (60) in Ref. [3]] the ferrite tube. As a consequence, after integration, Eq. (5) is valid both in the tube and on its surface. We conclude that the same emf is expected on the surface of the tube as inside the tube (both for $\rho = b$).

A severe critique of the above reasoning can be made since in the derivation of Eq. (63) in Ref. [3], use was made of the flux-diffusion equation, which depends on the material properties (Ohm's law) and thus may be invalid outside the tube. Instead, a rigorous procedure would use Eq. (1):

$$\mathcal{E} = \oint (\mathbf{E} + \mathbf{v} \times \mathbf{B}) \cdot \mathbf{dl}, \qquad (A13)$$

which does not contain any material parameters. Following Ref. [3] (see, e.g., Appendix A of Ref. [3]), the $\mathbf{E}$ field is conservative: "In general, the electric field seen in this frame [the frame K] is given by $\mathbf{E} = -\partial \mathbf{A}/\partial t - \nabla V$. However, for our nonrotating dipole [i.e. Earth's magnetic field], we can put $\partial \mathbf{A}/\partial t = 0$ so $\mathbf{E} = -\nabla V$." This implies that there is no contribution to the emf from $\mathbf{E}$. Hence, we focus on the $\mathbf{v} \times \mathbf{B}$ term and use the geometry of Fig. 1 in Ref. [3], but for a (similar) loop with legs d–e and f–g immediately on top of the ferrite [legs d–g and e–f could be in small cylindrical holes, or outside, at the sides of the tube; in any case $(\mathbf{v} \times \mathbf{B}) \perp \mathbf{dl}$ for these legs, so they do not contribute to the integral in Eq. (1)]. Since $B_y \hat{\mathbf{y}}//\mathbf{v}$, only

B_x contributes to the integral in Eq. (A13) for this loop and hence we find

$$\mathcal{E} = -\oint_C v B_x \hat{\mathbf{z}} \cdot d\ell; \qquad \text{(A14)}$$

that is, we recover Eq. (A3), and as a consequence also Eq. (2). Thus we have shown that within the argumentation in Ref. [3], Eq. (2) also holds for a wire loop that runs immediately above the tube, and thus that Eq. (5) can also be used for that geometry. Of course, the value of B_x, Eq. (A12b), outside the tube should be used. As discussed above, however, this value is equal to the value inside the tube (both for $\rho = b$). In conclusion, the same emf is expected for the loop inside the ferrite material, as used for the calculation in Ref. [3], and for a loop immediately on top of the tube, such as our copper loop discussed in Sec. V.

[1] R. E. Smalley, Future global energy prosperity: The terawatt challenge, MRS Bull. **30,** 412 (2005).

[2] S. Pacala and R. Socolow, Stabilization wedges: Solving the climate problem for the next 50 years with current technologies, Science **305,** 968 (2004).

[3] C. F. Chyba and K. P. Hand, Electric Power Generation from Earth's Rotation through Its Own Magnetic Field, Phys. Rev. Appl. **6,** 014017 (2016).

[4] H. Reichl and J. Wolf, in *True Visions*, edited by E. Aarts and J. Encarnação (Springer, Berlin, Heidelberg, 2006).

[5] S. J. Barnett, An investigation of the electric intensities and electric displacement produced in insulators by their motion in a magnetic field, Phys. Rev. (Ser. I) **27,** 425 (1908).

[6] S. J. Barnett, On electromagnetic induction and relative motion, Phys. Rev. **35,** 323 (1912).

[7] I. Newton, Principia, Book 1: Scholium (1686).

[8] E. Mach, *The science of Mechanics* (Open Court Publishing Company, Chicago London, 1919), p. 543.

[9] G. Sagnac, L'éther lumineux démontré par l'effet du vent relatif d'éther dans un interféromètre en rotation uniforme, Comptes Rendus **157,** 708 (1913).

[10] A. L. Kholmetskii, One century later: Remarks on the Barnett experiment, Am. J. Phys. **71,** 558 (2003).

[11] V. Leus and S. Taylor, On the motion of the field of a permanent magnet, Eur. J. Phys. **32,** 1179 (2011).

[12] Francisco J. Müller, Unipolar induction revisited: New experiments and the "edge effect" theory, IEEE Trans. Magn. **50,** 7000111 (2014).

[13] K. Chen, X.-J. Li, and Y.-X. Hui, An experimental study on unipolar induction, Acta Phys. Pol. A **131,** 271 (2017).

[14] D. J. Griffiths, *Introduction to Electrodynamics* (Prentice-Hall International (UK) Limited, London, 1999), 3rd ed.

[15] P. J. Scanlon, R. N. Henriksen, and J. R. Allen, Approaches to electromagnetic induction, Am. J. Phys. **37,** 698 (1969).

[16] E. M. Pugh, Conservative fields in dc networks, Am. J. Phys. **29,** 484 (1961).

[17] I. Galili, D. Kaplan, and Y. Lehavi, Teaching Faraday's law of electromagnetic induction in an introductory physics course, Am. J. Phys. **74,** 337 (2006).

[18] E. M. Purcell, *Electricity and Magnetism*, Berkeley Physics Course (Cambridge University Press, New York), Vol. II (1985), 2nd ed.

[19] I. Galili and D. Kaplan, Changing approach to teaching electromagnetism in a conceptually oriented introductory physics course, Am. J. Phys. **65,** 657 (1997).

[20] https://www.ngdc.noaa.gov/geomag-web/#igrfwmm (retrieved on 30 January 2018).

[21] http://www.fair-rite.com/product/round-cable-emi-suppression-cores-2675626402 (retrieved on 30 January 2018).

[22] http://www.fair-rite.com/75-material-data-sheet/ (retrieved on 30 January 2018).

[23] R. Gerber, Z. Šimša, and M. Vichr, Some physical properties of single crystal manganese ferrites, Czech. J. Phys. B **16,** 913 (1966).

[24] K. Latha and D. Ravinder, Electrical conductivity of Mn-Zn ferrites, Phys. Stat. Sol. (a) **139,** K109 (1993).

[25] M. L. Kidd, Watch out for those thermoelectric voltages! Cal Lab: Int. J. Metrol. **19,** 18 (2012).

[26] M. Harder, Y. Gui, and C.-M. Hu, Electrical detection of magnetization dynamics via spin rectification effects, Phys. Rep. **661,** 1 (2016).

[27] http://www.fair-rite.com/product/round-cable-emi-suppression-cores-2675102002 (retrieved on 30 January 2018).

[28] R. B. Goldfarb, in *Concise Encyclopedia of Magnetic and Superconducting Materials*, edited by J. Evetts (Pergamon Press, 1992), 1st ed.

[29] L. V. Bewley, *Flux Linkages and Electromagnetic Induction* (Dover, New York, 1964), p. 81.

[30] H. J. Boersma, *Elektromagnetisme (Lecture notes on Electromagnetism)* (Vrije Universiteit, Amsterdam, 1996), p. 255.

[31] For the electrical analogue, see problem 6.19 in Ref. [18] and its solution, which is oddly numbered 6.28 in the solution manual.

[32] R. P. Feynman, R. B. Leighton, and M. Sands, *The Feynman Lectures on Physics* (Addison-Wesley, New York, 1972).

[33] See p. II-26-9 in Ref. [32].

[34] See Eq. (12.108) in Ref. [14].

[35] A. K. T. Assis and F. M. Peixoto, On the velocity in the Lorentz force law, Phys. Teacher **30,** 480 (1992).

[36] J. Jeener, Refutation of [Chyba and Hand, Phys. Rev. Applied 6, 014017 (2016)]: No Electric Power can be Generated from Earth's Rotation through its Own Magnetic Field, arXiv:1712.04283v2.

[37] S. Chapman, The diurnal changes of the Earth's magnetism, Observatory **41,** 52 (1918).

[38] J. J. Love and E. J. Rigler, The magnetic tides of Honolulu, Geophys. J. Int. **197,** 1335 (2014).